Flexural performance of fire damaged and rehabilitated two span reinforced concrete slabs and beams

Jiang-Tao Yu*[1], Yuan Liu[1], Zhou-Dao Lu[1] and Kai Xiang[2]

*[1]Research Institute of Engineering & Disaster Reduction, Tongji University,
Siping Rd, Shanghai, 200092, China*
[2]Tianjin Fire Research Institution of the Ministry of Public Security, Weijin Rd, Tianjin, 300000, China

Abstract. Five two-span reinforced concrete (RC) slabs and seven two-span RC beams were tested under the ISO 834 standard fire with different durations. CFRP strengthening was then applied to some of the specimens after the damaged concrete was removed from the specimens and replaced with polymer mortar. All the specimens were loaded to failure to investigate the influence of fire-damage and the effectiveness of strengthening methods. Test results indicated that the flexural capacities of specimens decrease with the fire duration increases. Moreover, fire exposure had more significant effect on the flexural rigidity than on the bearing capacity of the specimens. After rehabilitation, the bearing capacities of specimens reached or even exceeded that of the reference RC specimen, and the strengthening methods seemed to have limited effect on flexural rigidity recovery. From the analysis of moment redistribution of tested beams, elevated temperature is found having different impacts on sagging moment region and hogging moment region. The damage of RC continuous member is definitely a comprehensive response of different regions.

Keywords: fire damage; concrete; continuous members; rehabilitation; flexural rigidity; bearing capacity

1. Introduction

Although severe fire may cause significant damage to reinforced concrete (RC) structures, collapse of RC structure, as the result of fire-damage, is rarely happened. Thus, an effective fire-damage evaluation method, serviced as the basis of rehabilitation, is always necessary for a fire-damaged RC structure.

In a compartment fire, slabs or beams, due to their spatial location, are likely to undergo the strongest thermal impact and be subjected to the most severe damage among all the structural members.

Compared with numerous investigations regarding the behavior of RC members in fire (Huang 2011, Choi and Shin 2011), relatively limited studies were directed towards the residual properties of RC members after fire. El-Hawary *et al.* (1996) performed experiments on the flexural strength of three RC simply supported beams and studied the impact of fire durations on the ultimate load

---

*Corresponding author, Ph.D., E-mail: yujiangtao@tongji.edu.cn

and deflection. Moreover, the shear strength of simply supported RC beams was found highly dependent on the fire durations and thicknesses of concrete cover (El-Hawary *et al.* 1997). Phani and Kumar (2010) tested twelve simply supported RC beams with different concrete grades, fire durations and stirrup spacings. The effect of fire duration was found to be the key factor by the authors. Five loaded RC beams were heated to 800ºC for 30 minutes by Kowalski and Krol (2010). The test results show that the residual bearing capacity of specimens decreased significantly with the failure mode of concrete crushing. Considering the extensive fire test, some analysis methods were proposed to model the residual mechanical properties of RC beams after fire exposure. Hsu and Lin (2008) used finite difference method to model the temperature history of RC beams subjected to fire. Additionally, the structural analysis, on the basis of lumped method, was performed to calculate the residual bending moment, shear strength and elastic modulus of RC beams after fire.

For simply supported RC members subjected to fire, tensile concrete is directly exposed to fire from underneath, while compressive concrete generally has little chance to a fire and will suffer much less damage than the tensile region. Considering tensile concrete normally contributes little to the flexural strength of slab or beam, softening of steel rebars at elevated temperatures is believed to be the crucial factor of strength degradation in such case. After fire, with the steel rebars regaining most of their strength at ambient temperature (Elghazouli *et al.* 2009), a simply supported RC member can recover considerably its initial flexural strength. As to continuous RC members, the situation will be different. The compressive concrete in the hogging moment region of continuous member has equal chance to be directly exposed to fire. Unlike the heat impact on steel rebar, fire damage on compressive concrete is unrecoverable and should not be neglected when evaluating damage level of RC members (Schneider 1988 and Bazant 1996). Additionally, compared with simply supported members, continuous RC members have much more extensive applications in actual practice. Therefore, continuous instead of simply supported slabs and beams are the subject investigated in this paper.

Over the past decade, numerous researchers concentrated on the strengthening of RC structures with externally bonded fiber-reinforced polymer (FRP) laminates. However, limited studies were concerned with the strengthening of fire-damaged RC members with FRP. Haddad *et al.* (2011) tested 16 high strength RC slabs (one-way) under four-point loading after heating them to 600ºC for two hours. The specimens were repaired with advanced composite materials, including steel fiber reinforced concrete layers, carbon fiber reinforced polymer (CFRP) sheets and glass fiber reinforced polymer (GFRP) sheets to investigate the coupling effects of water recurring and strengthening. An experimental study was undertaken by Yaqub and Bailey (2011) to investigate the axial capacity of post-heated circular reinforced concrete columns repaired with GFRP and CFRP sheets. The results indicated that strengthening with a single layer of unidirectional FRP has a significant effect on the axial strength and ductility of circular columns. However, the effect of a single layer of GFRP or CFRP sheets on the axial stiffness was not significant.

This paper focuses on the experimental test of the residual flexural performance of RC continuous slabs and beams after fire. Because the fire damage of RC flexural members could not automatically be recovered after fire, the effect of a novel FRP strengthening method is investigated for fire-damaged RC continuous beams.

2. Test arrangement

2.1 Design of specimens

Totally five two-span continuous slabs and seven two-span continuous beams were fabricated for the experimental investigations. Slabs with 2600 mm length in either span, were designed with a rectangular cross-section of 1200 mm × 120 mm and cast monolithically with three supported beams. The beams were designed as a *T* section with a total height of 300 mm and a web width of 200 mm. The flange is 900 mm in width and 80 mm in thickness. Both the slabs and the beams had two equal spans of 2600 mm. The details of specimens are summarized in Fig. 1 and Fig. 2.

The mix proportions of concrete were 1: 2.2: 3.1: 0.5 (cement: sand: gravel: water) for slabs and 1:2.7:3.7:0.6 for beams. After 28-day curing, tests on concrete prisms (100 mm × 100 mm × 200 mm) gave the average compressive strengths of 28.0 MPa for slabs and 34.6 MPa for beams at ambient temperature. The corresponding elasticity moduli were 2.94×10^4 MPa and 3.39×10^4 MPa,
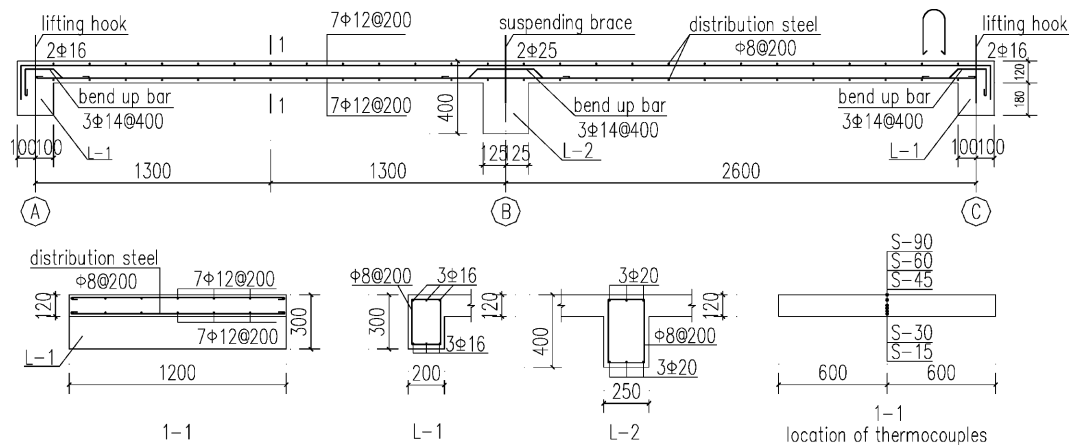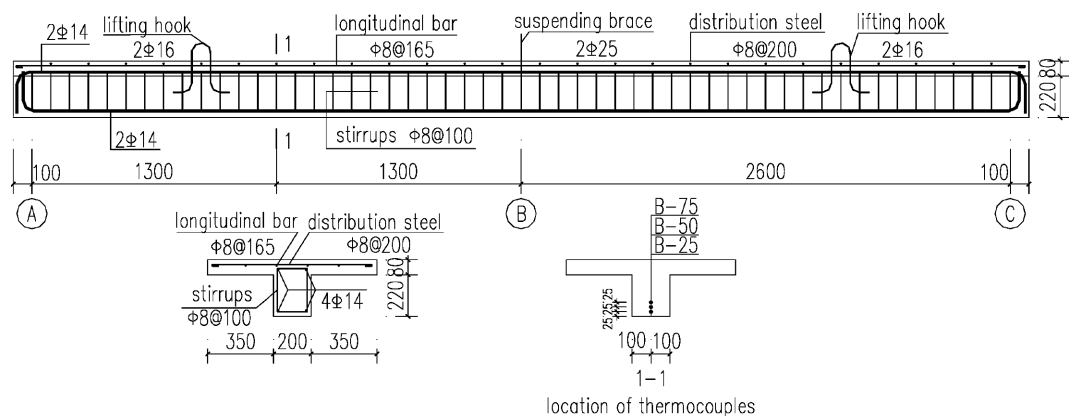

Fig. 1 Layout and dimension of slabs
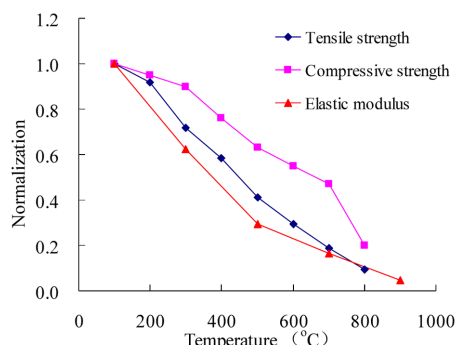

Fig. 2 Layout and dimension of beams

Fig. 3 Temperature-dependent reduction of concrete's material properties

respectively. The yield and ultimate strengths of steel rebars were 286 MPa and 408 MPa for slabs, and 364 MPa and 542 MPa for beams. The elasticity moduli of steel rebars were tested to be 2.15×105 MPa for slabs and 2.0×105 MPa for beams, respectively.

In the preceding test (Yu 2007), total 192 concrete primes were heated to various elevated temperatures. After cooling down, compressive tests (80 specimens) and splitting tests (112 specimens) were conducted to obtain the compressive strength, elasticity modulus and tensile strength. The mechanical properties of concrete are normalized by the values obtained at ambient temperature and the temperature-dependent relationships are shown in Fig. 3.

Due to the spatial location and sectional dimension, slabs generally undergo the most severe damage in a compartment fire. Beams or columns with larger section size and higher steel ratio usually suffer comparatively slighter damage. In the practical fire-damage evaluation of RC structures, structural engineers usually consider to demolish the severely damaged slabs but provide rehabilitation for the fire-damaged beams or columns. Thus, experiments in this paper focused on the fire impact on the residual mechanical properties of slabs. As to the beams, the effectiveness of strengthening methods was emphasized.

The tests involved three stages. First, expose the specimens, except the reference specimens S0 and L0, to ISO 834 standard fire (ISO/FDIS 834-1 1999) for different durations. Secondly, remove the damaged layer (only for specimens S1C, L2C, L3C, L5C and L6C), repair it with polymer mortar and then reinforce those specimens with CFRP sheets. Thirdly, load all the specimens to failure. The schedule of the tests was listed in Table 1.

Table 1 Test program

Member	Specimen Code	Fire Duration	Reinforcement Yes/No	Member	Specimen Code	Fire Duration	Reinforcement Yes/No
Slab	S0 (reference)	/	No	Beam	L0 (reference)	/	No
	S1	30 min	No		L1	60 min	No
	S1C	30 min	Yes		L2C	60 min	Yes
	S2	50 min	No		L3C	60 min	Yes
	S3	70 min	No		L4	75 min	No
	S4	100 min	No		L5C	75 min	Yes
					L6C	75 min	Yes

2.2 Fire test of the specimens

Fire tests were undertaken in a gas furnace at the fire laboratory of Tongji University. The test setup for slabs is shown in Fig. 4 and the same applies to the beams. All the specimens were heated from underneath, saying three-face fire exposure for beams and one-face fire exposure for slabs.

In Fig. 4, two ends of slab were supported by a roller pin support and a hinged support, respectively. Two precast steel rebars, acted as middle support, suspended the specimen in the entire process. Iron blocks were placed on the upper surface of slabs to apply a constant load of 1.0 kN/m². Linear variable displacement transducers (LVDTs) and thermocouples were employed to record the vertical displacement and temperature responses. The supporting regime for beam was similar.

All the specimens were exposed to the ISO834 standard fire. In the heating process, visual cracks, perpendicular to the longitudinal direction, were observed at the upper surface near the middle support. The formation of cracks was expected as the combined effects of temperature, support constraint and applied load. After fire, explosive concrete spallings, about 15 mm in depth, were observed at the soffit surfaces of slabs and beams, as shown in Fig. 5. The other observations about the fire tests, such as color variations and thermal deflections of test specimens, are not included in this paper.

Take slab S2 and beam L1 for example, the temperature histories are shown in Fig. 6. The number following the specimen number represents the location of thermocouple as shown in Fig. 1
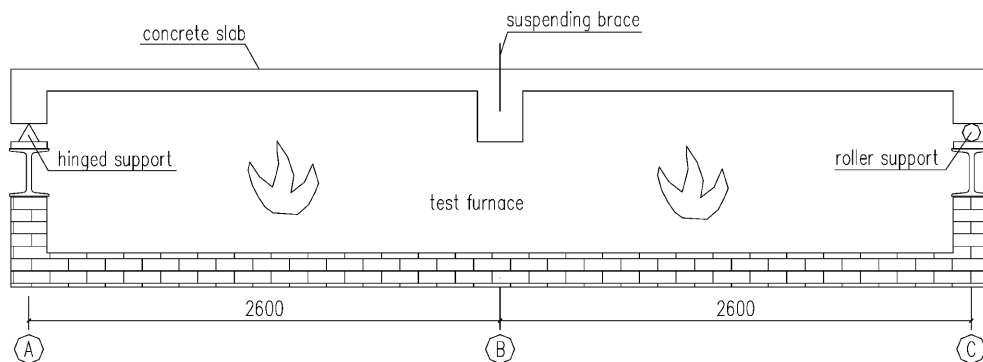

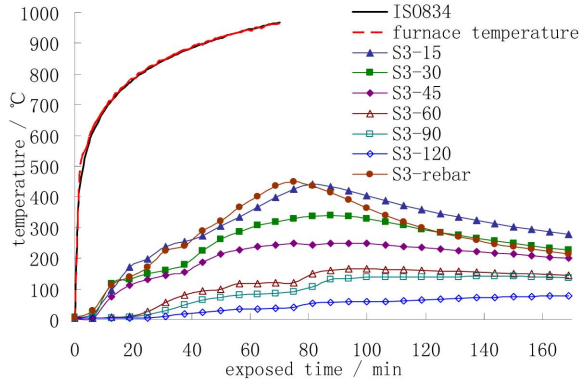Fig. 4 Fire test setup

Fig. 5 Spalling on the bottom of slab

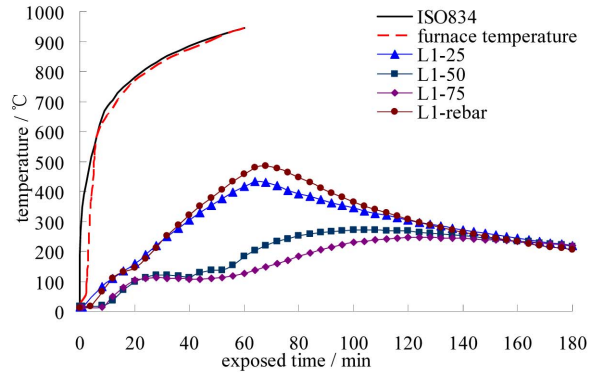Fig. 6 Temperature histories of S3   Fig. 7 Temperature histories of L1

and Fig. 2. Owing to water evaporating, platforms near 100ºC appeared in the heating processes. Because of the low thermal conductivity of concrete, there are time lags between the highest temperatures of furnace and concrete.

2.3 Strengthening methods of specimens after cooling down

S1 and S1C represented two individual spans of one specimen. S1C is a span randomly chosen for strengthening after fire. S1C, L2C, L3C, L5C and L6C were all strengthened at ambient temperature. To determine the damage thickness of concrete, a novel method of core drilling was employed. According to the reference literature (Yu 2007), transversal splitting was applied at the cross sections of cores in different depth, and revealed the variation of tensile strength, as shown in Fig. 8. A similar but not identical method was introduced by Dilek and Leming (2008). The damaged concrete with splitting strength degradation of more than 20% was removed and replaced with polymer mortar. Subsequently, those specimens were strengthened by externally bonded CFRP sheets. The strengthening details are listed in Table 2. The CFRP sheet with the nominal thickness of 0.111 mm has an average tensile strength and an elastic modulus of 3540.0 MPa and 243.0 GPa, respectively. The shear and tensile strengths of bonding adhesive were provided by the manufacturer as 26.0 MPa and 44.0 MPa, respectively.
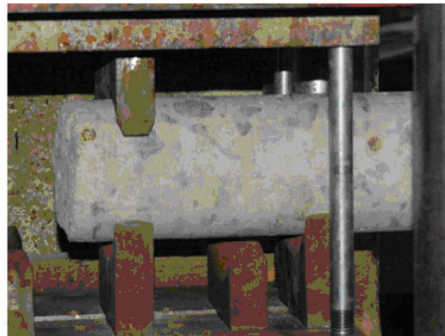

Fig. 8 Splitting in the depth direction

Table 2 Details of CFRP sheet strengthening

Specimens number	Top surface near middle support					Bottom surface at mid-span				
	Layers	Length (mm)	Width (mm)	Strips	Interval (mm)	Layers	Length (mm)	Width (mm)	Strips	Interval (mm)
S1C	1	1075	150	4	150	1	2375	150	2	100
								100	2	
L2C						1	2200	150	1	
L3C	1	1800	100	2	200	2	2200	150	1	
L5C	1	1800	150	2	200					
L6C						2	2200	150	1	

Note: For strengthening on the bottom surface of sagging moment region, strengthen one span for slab and double spans for beams.

In order to prevent peeling, 200 mm-wide CFRP U-wraps were applied to the beams with a interval of 200 mm. As to SC1, two strips of CFRP sheet, 200 mm in width, were pasted on both sides of strengthened regions as transverse anchorages.

2.4 Loading test

Concentrated loads were applied to the beams through two hydraulic jacks and steel girders, as shown in Fig. 9. The loading regime for slabs was similar. The load was gradually increased by successive 10 kN increments, which were progressively reduced near failure. LVDTs and strain gauges were used to measure the deflections and strains of the concrete and steel rebar. Two force transducers were placed under side supports to measure the counterforce of the supports.

Once the maximum deflection reached 1/50 of the length of span or the compressive concrete crushed, the ultimate bearing capacity is assumed to be reached and the test should be terminated (GB 50152-92: Standard Methods for Testing of Concrete Structures). For CFRP reinforced specimens, tensile rupture of CFRP sheet is also corresponding to ultimate bearing capacity. Additionally, the applied load corresponding to the mid-span deflection of 1/200 of span is taken as the criterion for serviceable bearing capacity (GB 50010-2010: Code for Design of Concrete Structures).

All the non-strengthened specimens behaved similarly during the tests. Taking S1 for example, the cracks on the top surface of sagging moment region, which formed in fire test, were observed propagating during loading. With the increase of applied load, flexural cracks initiated at the soffit surface of mid-span. In the post-loaded process, the deflection increased rapidly and the values of applied load kept almost constant, which proclaimed the approaching of flexural failure.

The experimental phenomena of CFRP reinforced specimens were similar to that of non-strengthened specimens at the beginning stage. Although the sounds of adhesive fracture were clearly heard in the later loading process, no visual debonding was observed in the tests. All the tests were ended with CFRP rupture. It should be noted that concrete crushing were observed in the hogging moment region of S4, L1 and L4 after loading. This phenomenon can be attributed to the dramatically lost of compressive strength of concrete in hogging moment region after fire.

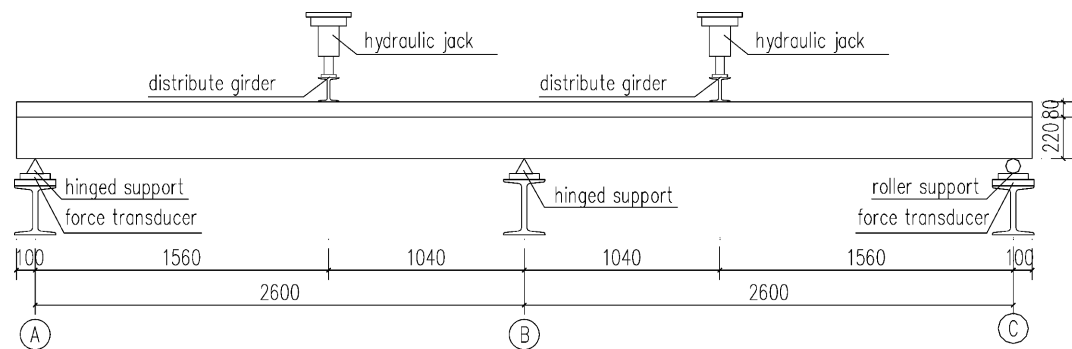The failure modes and corresponding descriptions were listed in Table 3.

Fig. 9 Static test set-up

Table 3 Failure model of specimens

Specimens number	Failure model	details description
S0	Flexural failure	Excessive deflection
S1	Flexural failure	Excessive deflection
S1C	CFRP sheet rupture	CFRP rupture in sagging moment region
S2	Flexural failure	Excessive deflection
S3	Flexural failure	Excessive deflection
S4	Flexural failure	Concrete crush in hogging moment region and excessive deflection
L0	Flexural failure	Excessive deflection
L1	Flexural failure	Concrete crush in hogging moment region
L2C	CFRP sheet rupture	CFRP rupture in sagging moment region
L3C	CFRP sheet rupture	CFRP rupture in hogging moment region
L4	Flexural failure	Concrete crush in hogging moment region
L5C	CFRP sheet rupture	CFRP rupture in hogging moment region
L6C	CFRP sheet rupture	CFRP rupture in sagging moment region

3. Discussion of the test results

3.1 Test results of slabs

Although specimens were cast and cured under the same laboratory conditions, there were still inevitable discrepancies among the specimens. Even the different spans of a same specimen were different in loading response. The span which firstly reached the ultimate state was called "weak span" in the following context. Hereafter, all the discussions are based on the test data within "weak span", except for S1 and S1C, of which both spans were loaded to failure to investigate the effectiveness of strengthening method.

The transverse deflections at mid-span of slabs are depicted in Fig. 10. Based on that, the following text will discuss the influence of fire durations on the basic mechanical properties, such as bearing capacity, initial rigidity, compressive strain of concrete and tensile strain of rebar and CFRP.
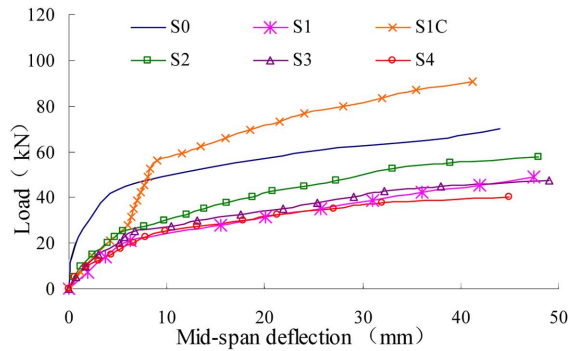
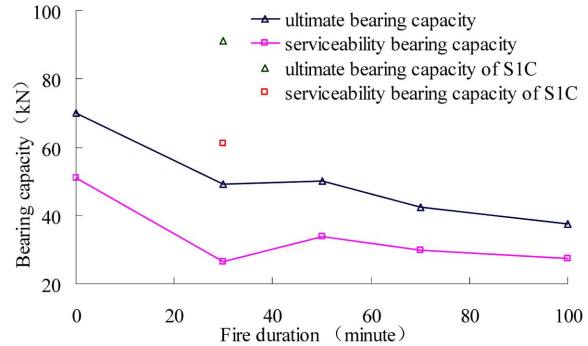Fig. 10 The load-deflection curves at mid-span of slabs

Fig. 11 Comparison of ultimate bearing capacity and serviceable bearing capacity between slabs

3.1.1 Bearing capacity

The decline rates of ultimate bearing capacity and serviceable bearing capacity are shown in Fig. 11. It is clearly seen that the bearing capacities drop significantly after fire. For instance, S4 reduces the ultimate bearing capacity and serviceable bearing capacity by 45% and 46% after 100 minutes fire exposure. Additionally, the decline rates of bearing capacities slow down with the increasing of fire durations.

As shown in Fig. 10 and Fig. 11, the ultimate and serviceable bearing capacities of S1C were fully recovered from degradation, which were respectively 30% and 20% higher than those of undamaged S0, meanwhile 86% and 131% higher than those of S1. It can be concluded the loss of bearing capacity have been effectively recovered by FRP strengthening.

3.1.2 Initial flexural rigidity

Table 4 illustrates the decline rates of slabs' initial flexural rigidity. Compared with bearing capacities, the initial rigidities decrease much more significantly. It should be noted that the CFRP reinforcement, which is highly effective in enhancing the bearing capacity, seems to have much less effect on the initial rigidity recovery.

3.1.3 Compressive stain of concrete

Fig. 12 shows the strains of concrete at the lower surface of the hogging moment region. The compressive strains of concrete, even at the beginning stage, are obviously larger than that of S0. Comparing the strains of S0 and S1C, the effect of damaged concrete replacement is limited at beginning but remarkable at the latter stage. The load-strain curves of concrete at the upper surface of sagging moment region are shown in Fig. 13. Although the concrete in the upper layer was not directly exposed to fire, there are still differences in strain response among specimens. This may be attributed to the variation of moment redistribution from the hogging moment region towards the middle support.

Table 4 The initial flexural rigidity of slabs

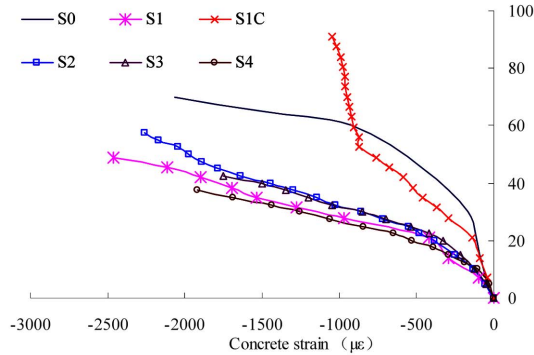| Specimen	S0	S1	S1C	S2	S3	S4
Normalization of initial flexural rigidity	1.00	0.10	0.15	0.17	0.14	0.10

Fig. 12 Load-strain curves of concrete at the bottom surface near the middle support
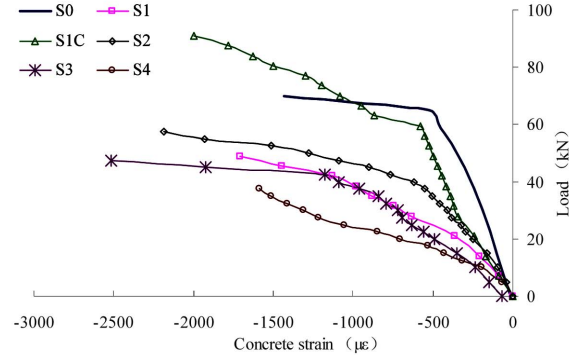

Fig. 13 Load-strain curves of concrete at the top surface of mid-span

3.1.4 Tensile stain of steel and CFRP

The tensile stains of steel rebars and CFRP sheets at the bottom of sagging moment region are plotted in Fig. 14. It is indicated the strains of fire damaged slabs, including S1C, increase obviously faster than that of S0 when loading. The steel rebars of S1, S2 and S4 yield when the applied loads are less than 30 kN, while the corresponding values of S0 and S1C are approximately 61.0 kN and 56.0 kN, respectively. The strain of CFRP sheets increases at a rapid rate after steel rebars yielding, then the CFRP sheet plays a major role in enhancing the bearing capacity.

3.2 Test results of beams

Similar to the slab tests, the loading tests of continuous RC beams were performed after fire exposure.
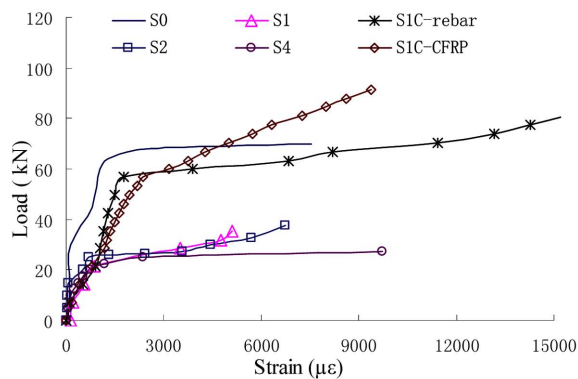

Fig. 14 Load-strain curves of steel rebars and CFRP at the bottom of sagging moment region of beams
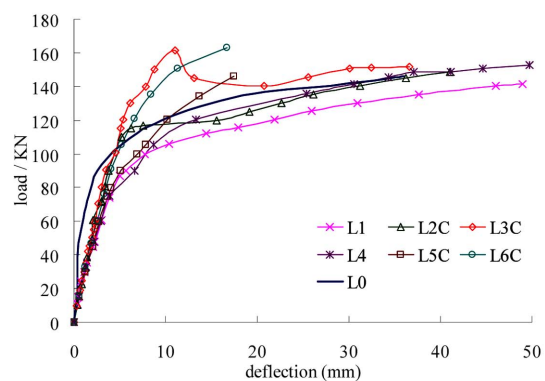

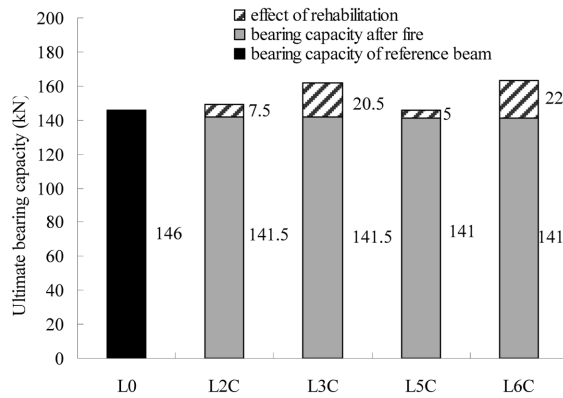Fig. 15 The load-deflection curves at the mid-span of beams
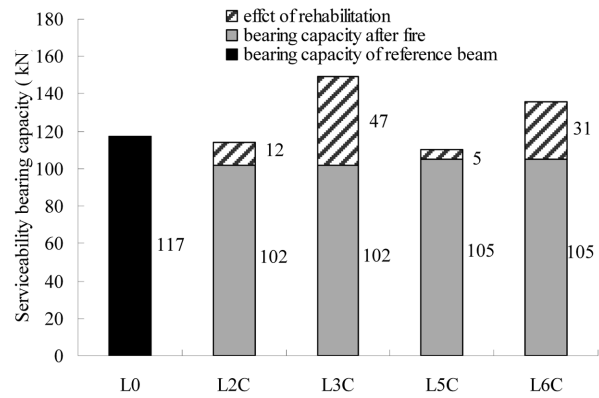
Fig. 16 Ultimate bearing capacities of beams

Fig. 17 Serviceable bearing capacities of beams

3.2.1 Bearing capacity

Fig. 15 presents the load-deflection curves at the mid-span of beams. Fig. 16 and Fig. 17 show the comparisons of bearing capacity among the test specimens. The ultimate and serviceable bearing capacities of fire damaged beams are only slightly lower than that of L0. In contrast to the obvious effect on slabs, the influences on beams are much weaker.

For rehabilitation, strengthened specimens are commonly stronger than referencing L0. Especially the serviceable bearing capacity benefits more from CFRP. The strengthening effects on L3C and L6C (two layers CFRP sheets on the bottom of mid-span) are better. The ultimate and serviceable bearing capacities of L3C are 14.5% and 46.1% greater than L1, both of which suffered an equal fire exposure of 60 minutes. The weakest effect is seen in L5C, which was strengthened with one layer CFRP sheet on the upper surface of middle support. It turns out to have minor increases of 3.5% for ultimate bearing capacity and 4.6% for serviceable bearing capacity.

3.2.2 Initial flexural rigidity

At the lower load level in Fig. 15, the initial flexural rigidities of fire damaged beams, including the rehabilitated specimens, are smaller than that of L0. After yielding of steel rebar, CFRP sheet plays a full role and results in a higher flexural rigidity than that of L0.

Table 5 lists the normalization of initial flexural rigidity. The values decrease much dramatically than the bearing capacities. Similarly, the CFRP strengthening has little effect on the recovery of rigidity.

3.3 Analysis of the test results

The test results indicate that the decline rate of flexural rigidity is apparently greater than that of

Table 5 The initial flexural rigidity of beams

Specimen	L0	L1	L2C	L3C	L4	L5C	L6C
Normalization of initial flexural rigidity	1.00	0.63	0.61	0.62	0.59	0.55	0.61

bearing capacity after fire. This can be attributed to the following aspects:

The first factor is the variation in mechanical properties of concrete. As shown in Fig. 3, the preceding test shows the residual elastic modulus suffers the largest degradation after elevated temperatures, which is followed by the tensile strength, and then the compressive strength. For instance, after the exposure of 700ºC, the elastic modulus, tensile strength and compressive strength of concrete are 16.5%, 19% and 47% of the values at ambient temperature. The larger degradation in elasticity modulus will surely lead to a larger degradation in flexural rigidity, especially in hogging moment region.

The second factor is the per-existing visual cracks before loading. Although most of cracks were located in the tension sides of specimens, Visual cracks, as the result of non-uniform temperature distributions, pre-loading and constraint conditions, will inevitably reduce the effective area of cross section, which at last lead to the decrease of flexural rigidity. On the contrary, visual cracks in the tensile sides generally have little effect on the ultimate bearing capacity of flexural member.

As to the reason that damage level in bearing capacity is different from slabs to beams even after similar fire exposure, the following factors are expected to be taken into account.

The temperature histories of specimens S3 and L1, of which the fire durations are 70 minutes and 60 minutes, is plotted in Fig. 6 and Fig. 7 (the location of thermocouples is plotted in Fig. 1 and Fig. 2). Because of the poor heat conductivity of concrete, temperature gradients in the cross section are fairly steep. For example, the maximum temperatures of L1 were 434ºC, 271ºC and 197ºC at the points 25 mm, 50 mm and 75 mm from the fire exposed surface. S3 experienced the maximum temperatures of 401ºC, 340ºC, 250ºC, 165ºC and 75ºC at the points of 15 mm, 30 mm, 45 mm, 60 mm and 120 mm from the exposed surface. Thicknesses of concrete layer undergoing temperature above 200ºC are 74 mm for L1 and 54 mm for S3, which means 25% of the L1's sectional height and 45% of S3's sectional height. Similarly, the thicknesses corresponding to 300ºC are 46 mm for L1 and 37 mm for S3, which means 15% and 31% of the sectional height respectively. Additionally, Fig. 3 shows that the concrete after exposed to the temperature of 300 ºC reduces its compressive strength by only 10%, tensile strength by 28.3% and elastic modulus by 37.6%. In the temperature of 200ºC, the degradations are only 5%, 8.3% and 18.8%, respectively. That means only 25% of beam's sectional area has a compressive strength reduce of no more than 5%, and 15% of the sectional area loses compressive strength of 10%. The comparatively larger section size and shorter fire durations (no more than 75 minutes) lead to less severe damage of beams.

It may be worth noting that there are gaps, as to the damage level, between a whole member and the local region of the member. Take the results of beams for example. From Fig. 16 and Fig. 17, we find the loss of beams' bearing capacities is no more than 10% even after 75 minutes fire exposure. It may be likely to draw the conclusion that beams were slightly damaged. Whereas, using the data of two force transducers placed under side supports, we can easily obtain the maximum values of moment both in beam's sagging and hogging moment regions. To make a reference, the elasticity-based flexural moment are also calculated based on the assumption that the flexural rigidity is uniform along the longitudinal direction. Fig. 18 illustrates the curves of deduced maximum moment and elasticity-based moment in sagging and hogging moment regions. Table 6 lists the values of bearing capacity (ultimate load L_u) and corresponding sagging moment (M_S) and hogging moment (M_H) of each beam.

In Fig. 18, the moment distribution of L0 is close to the elasticity-based value before the yielding of steel rebar, whereas the fire-damaged beams, even from the very beginning, possess apparently
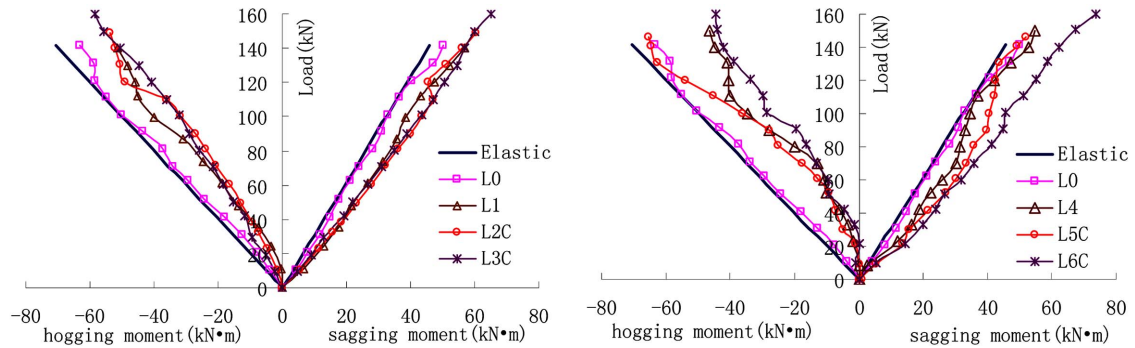
Fig. 18 Load versus flexural moment of beams

Table 6 Comparison of moment redistribution among beam specimens

Specimen number	M_H (kN·m)	Variation rate of M_H against L0	M_S (kN·m)	Variation rate of M_S against L0	L_u (kN)	Variation rate of L_u against L0
L0	-64.38	1.00	52.61	1.00	146	1.00
L1	-51.39	0.80	56.71	1.08	142	0.97
L2C	-53.74	0.83	60.58	1.15	149	1.02
L3C	-58.48	0.91	65.99	1.25	162	1.11
L4	-41.48	0.64	52.78	1.00	141	0.97
L5C	-65.21	1.01	51.96	0.99	146	1.00
L6C	-46.72	0.73	73.82	1.40	163	1.12

bigger moment in the sagging moment region and smaller moment in the hogging moment region than L0. That means the hogging moment region of fire-damaged beams can resist much less flexural bending moment than that of L0. The excessive moment is transferred to the sagging moment region. This can be attributed to the uneven effect of fire on the sagging moment region and hogging moment region. The hogging moment region had its compressive concrete exposed to fire, and suffered more severe degradation both in flexural rigidity and flexural strength. While the sagging moment region only had its tensile concrete subjected to fire, and naturally got much less damage. Table 6 also lists the variation rates of M_H, M_S and L_u against the corresponding values of *L0.* It can be seen clearly the difference from sagging moment region to hogging moment region of the same specimen. What's more, neither the variation in sagging moment region, nor that in hogging moment region can reflect solely the damage of the whole specimen. The flexural performance of a fire damaged beam is combined action of force, moment and deformation in both the sagging and hogging moment regions.

4. Conclusions

This paper presents an experimental study on the effects of fire on the flexural performance of two-span slabs and beams. The conclusions are summarized as follows:

(1) Elevated temperature has significant effect on the flexural performance of RC continuous members. The ultimate and serviceable bearing capacities of RC continuous member decrease with the increase of fire durations. Longer fire duration leads to larger damage.

(2) The initial flexural rigidity of RC continuous member drops much more dramatically than the bearing capacity after fire exposure.

(3) Damaged concrete repair and CFRP sheet strengthening can effectively enhance the bearing capacity of fire-damaged RC members. Nevertheless, the effect is limited in flexural rigidity recovery.

(4) From the analysis of moment redistribution of tested beams, elevated temperature is found having different impacts on sagging moment region and hogging moment region of RC continuous member. The damage of RC continuous member is definitely a comprehensive response of different regions.

Acknowledgments

References

Bazant, Z.P. and Kaplan, M.F. (1996), "Concrete at high temperatures", *Material Properties and Mathematical Models*, Longman Group Ltd.

Choi, E.G. and Shin, Y.S. (2011), "The structural behavior and simplified thermal analysis of normal-strength and High-strength concrete beams under fire", *Eng. Struct.*, **33**, 1123-1132.

Dilek, U. and Leming, M.L. (2008), "Elastic dynamic Young's modulus and permeability of concrete in fire damaged structural members", *J. Mater. Civil Eng.*, **20**(2), 102-110.

El-Hawary, M.M., Ragab, A.M., El-Azim, A.A. and Elibiari, S. (1996), "Effect of fire on flexural behavior of RC beams", *Constr. Build. Mater.*, **10**(2), 147-150.

El-Hawary, M.M., Ragab, A.M., El-Azim, A.A. and Elibiari, S. (1997), "Effect of fire on shear behavior of RC beams", *J. Appl. Fire Sci.*, **65**(2), 281-287.

Elghazouli, A.Y., Cashell, K.A. and Izzuddin, B.A. (2009), "Experimental evaluation of the mechanical properties of steel reinforcement at elevated temperature", *Fire Safety J.*, **44**(6), 909-919.

GB 50010-2010 (2010), *Code for Design of Concrete Structures*, Ministry of Construction, P.R. China. (in Chinese)

GB 50152-92 (1992), *Standard Methods for Testing of Concrete Structures*, Ministry of Construction, P.R. China. (in Chinese)

Haddad, R.H., AL-Mekhlafy, N. and Ashteyat, A.M. (2011), "Repair of heat-damaged reinforced concrete slabs using fibrous composite materials", *Constr. Build. Mater.*, **25**, 1213-1221.

Hsu, J.H. and Lin, C.S. (2008), "Effect of fire on the residual mechanical properties and structural performance of reinforced concrete beams", *J. Fire Prot. Eng.*, **18**(4), 245-274.

Huang, Z.H. (2011), "The behaviour of reinforced concrete slabs in fire", *Fire Safety J.*, **45**, 271-282.

ISO/FDIS 834-1 (1999), *Fire-resistance Tests -Elements of Building Construction*, Part 1 General Requirements.

Kowalski, R. and Krol, P. (2010), "Experimental examination of residual load bearing capacity of RC beams heated up to high temperature", *Structures in Fire - Proceedings of the Sixth International Conference,*

Michigan, June.

Phani Prasad, D.M.S., Kumar, V., Sharma, U.K. and Bhargava, P. (2010), "Moment curvature relationships for fire damaged reinforced concrete sections", *Structures in Fire - Proceedings of the Sixth International Conference*, Michigan, June.

Schneider, U. (1988), "Concrete at high temperatures—a general review", *Fire Safety J.*, **13**(1), 55-68.

Yaqub, M. and Bailey, C.G. (2011), "Repair of fire damaged circular reinforced concrete columns with FRP composites", *Constr. Build. Mater.*. **25**, 359-37.

Yu, J.T. (2007), "Experimental and theoretical research on damage assessment of reinforced concrete member after fire", Tongji University, Shanghai. (in Chinese)